Melt Rheology and Morphology of Physically Compatibilized Natural Rubber–Polystyrene Blends by the Addition of Natural Rubber-*g*-Polystyrene

R. ASALETHA,[1] G. GROENINCKX,[2] M. G. KUMARAN,[3] SABU THOMAS[1]

[1]School of Chemical Sciences, Mahatma Gandhi University, Priyadarshini Hills P.O., Kottayam-686 560, Kerala, India

[2]Laboratory of Macromolecular Structural Chemistry, Department of Chemistry, Katholeike University of Leuvan, Belgium

[3]Rubber Research Institute of India, Kottayam-686 009, Kerala, India

Received 12 August 1997; accepted 10 March 1998

ABSTRACT: Blends of natural rubber (NR) and polystyrene (PS) were prepared by melt mixing in a Brabender plasticorder and by solution casting using chloroform as the casting solvent. Earlier studies have indicated that these blends are incompatible and immiscible, and their compatibility can be improved by the addition of a graft copolymer of NR and PS (NR-*g*-PS). The rheological behavior of these blends has been carried out in the presence and absence of the compatibilizer using a capillary rheometer and a melt flow indexer. The effects of blend ratio, processing techniques (melt mixing versus solution casting), shear stress, and temperature on the rheological behavior have been studied in detail. Both in the presence and absence of the copolymer, the blends showed a decrease in viscosity with an increase of shear stress, indicating pseudoplastic nature. Solution-cast blends showed a higher viscosity as compared to melt-mixed blends. The viscosity versus composition curve of both melt-mixed and solution-cast blends showed negative deviation from the additivity at a higher shear rate region. This is associated with the interlayer slip between the highly incompatible NR and PS phases. The effects of graft copolymer loading and temperature on solution-cast blends were studied, and it was found that as the copolymer loading increases, the shear viscosity increases. This is due to the high interfacial interaction between the two components in the presence of the copolymer. The copolymer, in fact, locates at the interface and makes the interface more broad. However, at higher loading of the copolymer, the viscosity of the blends decreases. This may be associated with the formation of micelles, which have a plasticizing action on the viscosity of the blends. Melt elasticity parameters like principal normal stress difference, recoverable elastic shear strain, and die swell were evaluated. Master curves have been generated using modified viscosity and shear rate functions that contain the melt flow index as a parameter. The extrudate morphology of the blends was studied using a scanning electron microscope. Addition of the copolymer reduces the domain size of the dispersed phase, followed by a leveling off at a higher concentration. The leveling off is an indication of interfacial saturation. The interparticle distance also decreased followed by a leveling off at a higher loading of the copolymer. J Appl Polym Sci 69: 2673–2690, 1998

Key words: natural rubber; polystyrene; extrudate; morphology; rheology

Correspondence to: S. Thomas.

Journal of Applied Polymer Science, Vol. 69, 2673–2690 (1998)
 CCC 0021-8995/98/132673-18

INTRODUCTION

Blends of natural rubber (NR) and polystyrene (PS) are a relatively new class of thermoplastic elastomers (TPEs), which combine the superior processing characteristics of PS and the very good elastic properties of NR. NR–PS blends can be prepared either by the solution casting technique or by the melt mixing technique in an internal mixer. Since the blend is an incompatible one, the overall performance of the same can be improved by the addition of a suitable compatibilizer. Our earlier studies[1] indicated that a graft copolymer of NR and PS (NR-*g*-PS) acts as an efficient compatibilizer in NR–PS blends.

Melt flow studies of polymers are of great importance in optimizing the processing conditions and in designing processing equipments like injection molding machines, extruders, and dies required for various products. During the processing, the polymer or the blend may undergo various changes. Better knowledge of the processing faults and defects will help to introduce the suitable remedies to optimize the processing problems.[2] Melt rheological studies give us valuable viscosity data that will be helpful in optimizing the processing conditions. Parameters like melt viscosity as a function of shear rate or shear stress and temperature have become more and more important. NR and PS possess different melt viscosities, and in order to standardize the processing conditions for their blends, it is necessary to study the effect of shear stress at different temperatures on the viscosity. Hence, the effect of blend composition, temperature, shear stress, and compatibilizer loading on shear viscosity was studied. Melt elastic parameters like die swell, principal normal stress difference, and recoverable shear strain are essential parameters to explain the ultimate properties of the products that can be prepared from the blend.

A large number of studies have been reported on the melt flow behavior of elastomers and their blends. For example, Danesi and Porter[3] reported on the rheology–morphology relationships in the blends of isotactic polypropylene and ethylene propylene rubbers. Akhtar et al.[4] reported on the rheological behavior and extrudate morphology of thermoplastic elastomers from NR and high-density polyethylene (HDPE) with reference to the effects of blend ratio, dynamic crosslinking, and carbon black filler. The morphology was found to depend on the blend ratio and shear rate. Gupta et al.[5] have studied the various rheological aspects of blends of polypropylene with acrylonitrile butadiene styrene (ABS) and low-density polyethylene (LDPE) and correlated it with the morphology studies. Melt rheological behavior of natural rubber–ethylene vinyl acetate copolymer blends was studied by Koshy et al.[6] The morphology–rheology relationship of miscible and immiscible blends of ABS with poly(methyl methacrylate) (PMMA) was studied using ABS having different acrylonitrile (AN) content and PMMA with different molecular weights.[7]

Rheological properties of dynamically cured ethylene–propylene–diene monomer rubber (EPDM)–polypropylene–HDPE ternary blends were analyzed by Ha.[8] It was found that the curing agent has influence on the melt viscosity especially in blends of EPDM-rich compositions. The effect of shear intensity on the melt viscosity of dynamically cured EPDM-rich ternary blends were also investigated.

Melt rheological properties of PS–PE blend were studied by Vanoene.[9] Rheology and processing of olefin-based thermoplastic vulcanizates was studied by Goettler and coworkers,[10] with special emphasis on extrudate swell properties.

The rheological behavior of compatibilized blends has also been analyzed by various researchers. The influence of a compatibilizer (polypropylene-*b*-polyamide) in polypropylene–polyamide blends on the rheological properties was analyzed by Germain and coworkers.[11] A dual flow behavior has been observed in the system; that is, at low shear rate, the blend viscosity is higher than the viscosity of the matrix, while at a high shear rate, the contrary is observed. The low shear rate behavior has been analyzed, and a good agreement was found for low concentration blend. Studies were reported by Gupta and Purwar[12] on the melt rheological behavior of some ternary (compatibilized) and binary blends of polypropylene with one or two of the following polymers, that is, styrene-*b*-ethylene butylene-*b*-styrene triblock copolymer, PS, and LDPE. Rheological properties of blends of nylon-12-modified polypropylene were studied by Valenza and Acierno.[13] In this study, both maleic anhydride and acrylic-acid-modified polypropylene (PP-MAH and PP-ACR) were used. The rheological studies reveal that PP-MAH is more effective than PP-ACR. The effect of compatibilizer (maleic-anhydride-grafted styrene ethylene–butylene styrene block copoly-

mer) on the rheological properties of polyamide-6–polypropylene was studied in detail by Miettinen and coworkers.[14]

Joshi et al.[15] reported on the rheological aspects of poly(butylene terephthalate)–high-density polyethylene with a polyethylene-based ionomer as the compatibilizer. Measurements showed that shear viscosity increased for the blend with the addition of the compatibilizer and explained this behavior on the basis of theory of emulsions.

Rheological evolution of PS–PE blends was carried out by Utracki and Sammut.[16] The dynamic shear behaviors of LDPE, PS, LDPE–PS blends were studied, and a series of blends with hydrogenated poly(styrene-*b*-isoprene) diblock as the compatibilizer were also investigated. Recently, in this laboratory, the melt rheological behavior of NR–PMMA blends has been investigated in the presence and absence of a compatibilizer. The relationship between morphology and rheology has been established.[17]

TPEs from blends of NR and PS are a new class of materials, which will combine the positive aspects of both NR and PS. NR is characterized by good elastic properties, good resilience, and good damping behavior but poor chemical resistance and processability. On the other hand, PS exhibits its superior processing characteristics even though it is extremely brittle. The NR–PS blends exhibit good processability, impact strength, good flexibility, and a rubbery nature. However, to our knowledge, to date, no detailed study has been made on the morphology and properties of NR–PS blends. In the present work, we report on the rheological behavior of NR–PS blends with and without the addition of the compatibilizer (NR-*g*-PS). Melt flow characteristics such as shear viscosity, flow behavior index, melt elasticity, and extrudate deformation have been studied with special reference to the effect of blend ratio, compatibilizer loading, temperature, shear stress, and blending conditions. The elasticity parameters like principal normal stress difference and recoverable elastic shear strain were calculated, and the extrudate morphology of the blends has been analyzed. The role of the compatibilizer on the morphology and processing behavior of the blends has been discussed. Finally, master curves were generated using the modified viscosity and shear rate functions that contain the melt flow index as a parameter.

Table I Characteristics of the Materials Used

Material	Density (g/cm^3)	Solubility Parameter $(cal/cm^3)^{1/2}$	Molecular Weight (M_n)
NR	0.90	7.75	7.79×10^5
PS	1.04	8.56	3.51×10^5
NR-*g*-PS	—	—	3.95×10^5
$CHCl_3$	—	9.3	—

EXPERIMENTAL

Materials

Polystyrene was supplied by Poly Chem Ltd., Bombay, India. Natural rubber (ISNR-5) was supplied by Rubber Research Institute of India, Kottayam. The compatibilizer was prepared in our laboratory. The details of the material characteristics are given in Table I.

Preparation of the Compatibilizer

Natural rubber latex of known dry rubber content (DRC) was mixed with styrene emulsion and exposed to ^{60}Co-γ-radiation for 16 h (0.1166 M Rad/min).[1,18] The irradiated product was coagulated with 2% formic acid, washed with water, and dried in the oven. Homopolymers NR and PS were removed from the crude sample by soxhlet extraction with petroleum ether and methyl ethyl ketone, respectively.

Graft copolymer (NR-*g*-PS) was characterized by Fourier transform infrared (FTIR) spectroscopy, ^{1}H nuclear magnetic resonance (NMR) spectroscopy, and gravimetric methods. The grafting efficiency and percentage of PS grafted were 49 and 20%, respectively.[1,19]

The FTIR spectrum of the graft copolymer (Fig. 1) shows peaks at 3026 and 2855 cm^{-1}, which correspond to aromatic C—H stretching in PS.[1] Peaks at 1601 and 1541 cm^{-1} correspond to C═C stretching of aromatic ring of PS. A strong peak at 698 cm^{-1} stands for the monosubstituted benzene ring along with the characteristic absorptions of the NR group at 837 and 889 cm^{-1}. The peaks at 1452 and 1375 cm^{-1} correspond to the aliphatic C—H stretching in NR.

The ^{1}H-NMR spectrum of the graft copolymer obtained at 90 MHz shows chemical shifts at 1–2, 4.6–4.8, and 6.6 ppm, corresponding to alkyl pro-

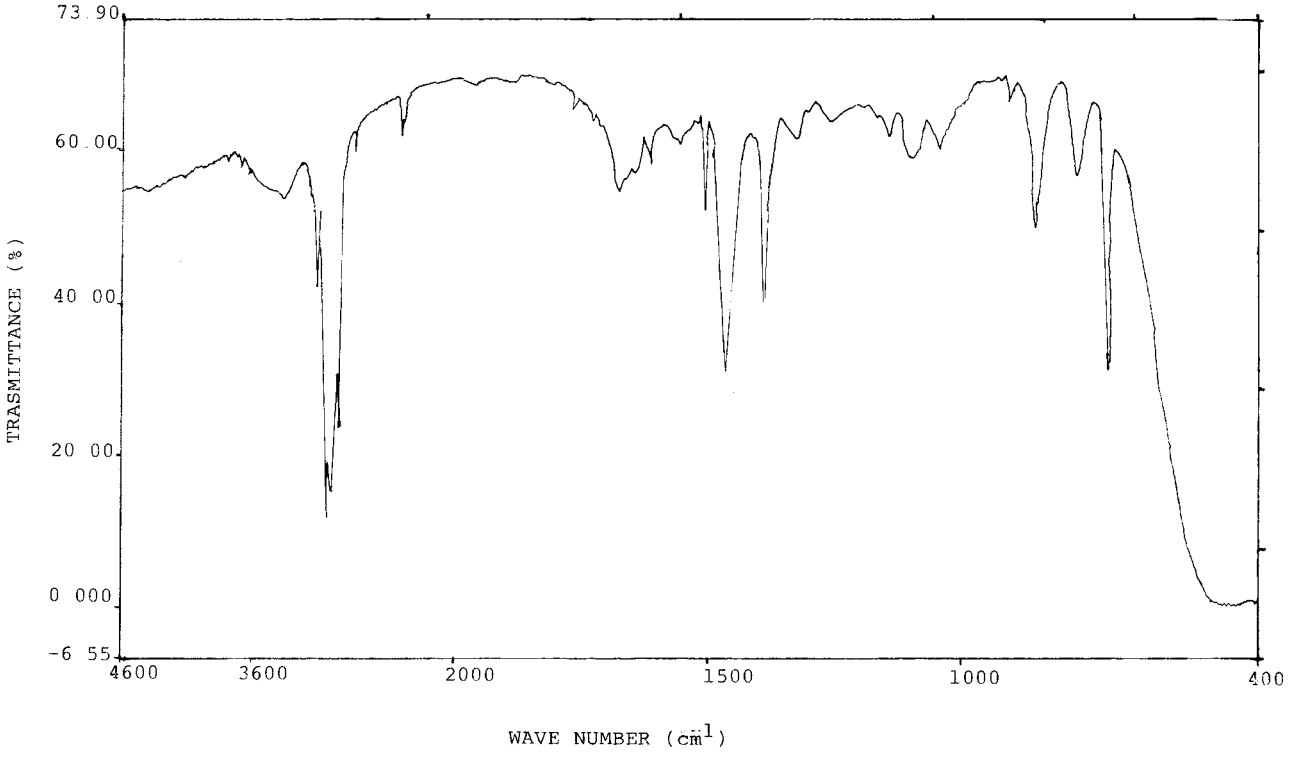

Figure 1 FTIR spectrum of NR-*g*-PS.

tons of NR, vinyl protons, and aromatic protons of PS, respectively.[1]

Preparation of Blends

Blends of NR and PS were prepared by melt mixing and the solution casting techniques. Melt mixing was carried out in a Brabender plasticorder (T 300A Model) at 160°C by maintaining the rotor speed at 80 rpm. At the start, PS was allowed to soften for 2 min, then NR was added. Total mixing time in all the cases was fixed as 9 min. The molten mix was then sheeted out in a cold press. Sample was cut into small pieces and used for melt rheology measurements. Blends were also prepared by the solution casting technique by dissolving the homopolymers in a common solvent ($CHCl_3$). Films were casted on a glass plate and then dried in the vacuum oven for the complete removal of the solvent.

The melt mixed samples are denoted by M_0, M_{30}, M_{50}, M_{70}, and M_{100}, and solution casted samples are denoted by S_0, S_{30}, S_{50}, S_{70}, and S_{100}. The subscripts correspond to the weight percentage of NR in the mixes. SG(a), SG(b), SG(c), and SG(d) correspond to the S_{50} blend, which contains 1.5, 3, 4.5, and 6 wt % NR-*g*-PS as a compatibilizer (Table II).

Rheological Measurements

The rheological measurements were carried out using viscotester (1500 version 2.0 model). A capillary die of length-to-diameter (l_d/d_c) of 30 was used, and the melts were extruded at 150, 160, and 170°C for different piston speeds. The test sample was placed inside the barrel of the extrusion assembly and forced down into the capillary with the piston attached to the moving crosshead. After a warming up period of 4 min, the melt was extruded through the capillary at preselected speeds of the crosshead, which varied from 0.02 to 2 mm s^{-1}. The height of the melt within the barrel was kept the same in all the experiments. Force corresponding to different piston speeds was recorded using a strip chart recorder assembly. The force and crosshead speed were converted into shear stress (τ_w) and shear rate ($\dot{\gamma}_w$) at wall, respectively, using the following equations involving the geometry of the capillary and piston:

Table II Composition of NR–PS Blends

Blend Code	M_0	M_{30}	M_{50}	M_{70}	M_{100}	S_0	S_{30}	S_{50}	S_{70}	S_{100}	$SG_{(a)}$	$SG_{(b)}$	$SG_{(c)}$	$SG_{(d)}$
Wt % of NR	0	30	50	70	100	0	30	50	70	100	50	50	50	50
Wt % of PS	100	70	50	30	0	100	70	50	30	0	50	50	50	50
Wt % of graft	0	0	0	0	0	0	0	0	0	0	1.5	3	4.5	6.0

$$\tau_w = \frac{F}{4A_p(1_c/d_c)} \tag{1}$$

$$\dot{\gamma}_w = \frac{(3n' + 1)}{4n'} \frac{32Q}{\pi d_3^c} \tag{2}$$

where F is the force applied at a particular shear rate. A_p is the cross-sectional area of the piston, l_c is the length of the capillary die, d_c is the diameter of the capillary, and Q is the volume flow rate. Q is calculated from the velocity of the crosshead and diameter of the plunger. The term n' is the flow behavior index, which is given by

$$n' = \frac{d(\log \tau_w)}{d(\log \dot{\gamma}_{wa})} \tag{3}$$

and was determined by the regression analysis of the values of τ_W and $\dot{\gamma}_{wa}$ obtained from the experimental data. The shear viscosity (η) was calculated as

$$\eta = \frac{\tau_w}{\dot{\gamma}_w} \tag{4}$$

Die Swell Measurements

The extrudates from the capillary were collected carefully without any deformation. The diameter of the extrudate was measured using an optical microscope (Model Leitz-Diaplan). An average of 10 readings was taken as the diameter (d_c) of the extrudate. Die swell was calculated as the ratio of the diameter of the extrudate to that of the capillary (d_e/d_c).

Extrudate Morphology Analysis

Morphology analysis of the extrudate was carried out by etching the minor blend phase using suitable solvents. The cryogenically fractured extrudate was immersed in petroleum ether for 48 h for the preferential extraction of NR and in methyl ethyl ketone for the extraction of PS. The samples were then dried in an air oven, and the extracted surface was examined with a scanning electron microscope (Philips). The surface characteristics of the extrudates at different shear rates were studied by optical microscopy.

Melt Flow Index

Melt flow index (MFI), that is, the weight of polymer in grams extruded in 10 min through a capillary, was determined using Ceast modular flow index (Model 6542/000) as per ASTM-D 1239-73. The applied load in all the cases was 2.16 kg. The measurement was carried out at 250°C.

RESULTS AND DISCUSSION

Effect of Shear Stress and Blend Ratio on Viscosity

Figure 2 shows the flow curves of NR–PS blends made by the solution casting technique using chloroform as the casting solvent. As shear stress increases, the viscosity decreases in all cases, indicating the pseudoplastic flow behavior. At zero shear, the molecules are randomly oriented and highly entangled and therefore exhibit high viscosity. Under the application of shearing force, the polymer chains orient, resulting in the reduction of shear viscosity and thus exhibit pseudoplastic behavior. The reduction in viscosity of the blends at higher shear rate is also due to the decrease in the particle size of the dispersed domains. During extrusion, the dispersed particles under the action of shearing force may undergo deformation, which further leads to the break down of the particles (Fig. 3). Figure 3(a,b) corresponds to noncompatibilized 50/50 NR–PS blends, and Figure 3(c,d) shows the corresponding compatibilized blends at two different shear rates, 57.6 and 115.2 s^{-1}, respectively. It was found that the average domain diameter was reduced from 0.781 to 0.361 μm as we increase the shear rate

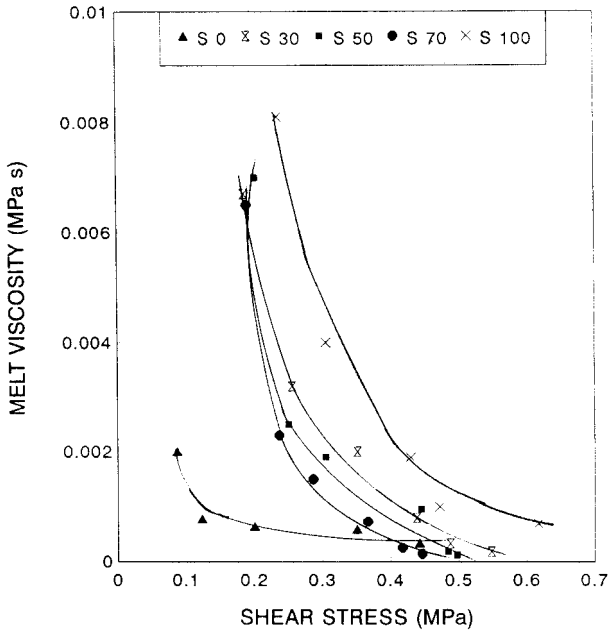

Figure 2 Variation of shear viscosity with shear stress of solution-cast blends.

from 57.6 to 115.2 s^{-1}. The domain diameter was found to be decreased upon compatibilization. The average domain diameter of 50/50 NR–PS blends was 24.77 and 18.91 μm at 57.6 and 115.2 s^{-1}, respectively. Upon compatibilization, the average domain diameter was reduced to 8.47 and 5.18 μm at 57.6 and 115.2 s^{-1}, respectively. The domain distribution of the blends at different shear rates are given in Figure 4. It is seen that as the shear rate increases, the distribution curves narrow down, indicating a fine distribution of the particles. This is further supported by the polydispersity index values, which are given in Table III. According to Munstedt[20] at a low shear rate, the dispersed plastic phase will form a wall structure around the rubber matrix. As the stress exceeds a minimum called yield stress, this wall structure breaks down, and viscosity decreases. Therefore, it is reasonable to believe that the decrease in viscosity with increase of shear stress is also due to the shearing away of the dispersed phase of the blend.

The flow (Fig. 1) curves indicate that the viscosity of the blends are nonadditive functions of the viscosities of NR and PS. This can be well understood from the variation of viscosity with the weight percentage of NR at low and high shear rates (both melt mixed and solution casted), as presented in Figure 5. NR always exhibits a slightly higher viscosity as compared to PS. At a lower shear rate, the viscosities of the blends are higher than those of the homopolymers. At the low shear region ($\leq$60 s^{-1}) up to 50 wt % NR, the viscosity of the blends increases and, thereafter, it decreases. In the region up to 50 wt % NR, there may arise strong interactions among the dispersed NR domains. This leads to the clustering of the domains. As a consequence, a reversible structural buildup arises, which leads to an increase in viscosity. This sort of positive deviation in the viscosity of polymer blends has been reported by many researchers.[21–24] An increase in viscosity at a lower shear region in the case of elastomer-modified thermoplastics has been reported by Lee.[22] Ablasova[23] reported that the viscosity of polyoxymethylene (POM)–copolyamide (CPA) goes through a maximum at low shear stress level and through a minimum at high shear stress level. On the other hand, in this system, a negative deviation is observed at the high shear rate region (Fig. 5). This is because at a high shear rate, the structure breaks down, and the interaction between the dispersed NR domains are reduced. Khanna and Congdon[25] also reported a reduction in viscosity in the case of PVC–hytrel blends. The negative deviation at a high shear rate can also be explained based on interlayer slip between NR and PS since the NR–PS blend is an incompatible system and it exhibits a two-phase morphology with large domains [Fig. 3(a,b)]. Upon compatibilization, the copolymer locates at the blend interface. As a result, the dispersed domain size decreases, which is an indication of interfacial saturation [Fig. 3(c,d)]. In the absence of the compatibilizer, the interface is highly mobile, weak, and unstable. This is schematically represented in Figure 6(a). Therefore, the application of shear force leads to high extent of inter layer slip between the phases, and this results in a viscosity that is lower than those of the component polymers.

The experimental viscosity data can be compared with the theoretical values calculated by various models. According to Utracki and Sammut,[16] positive or negative deviation of the experimentally measured viscosity from the theoretically calculated (log additivity rule) one is an indication of strong or weak interactions between the phases of the blend. According to this,

$$\ln (\eta_{app})\text{blend} = \sum_i W_i \ln (\eta_{app})i \qquad (5)$$

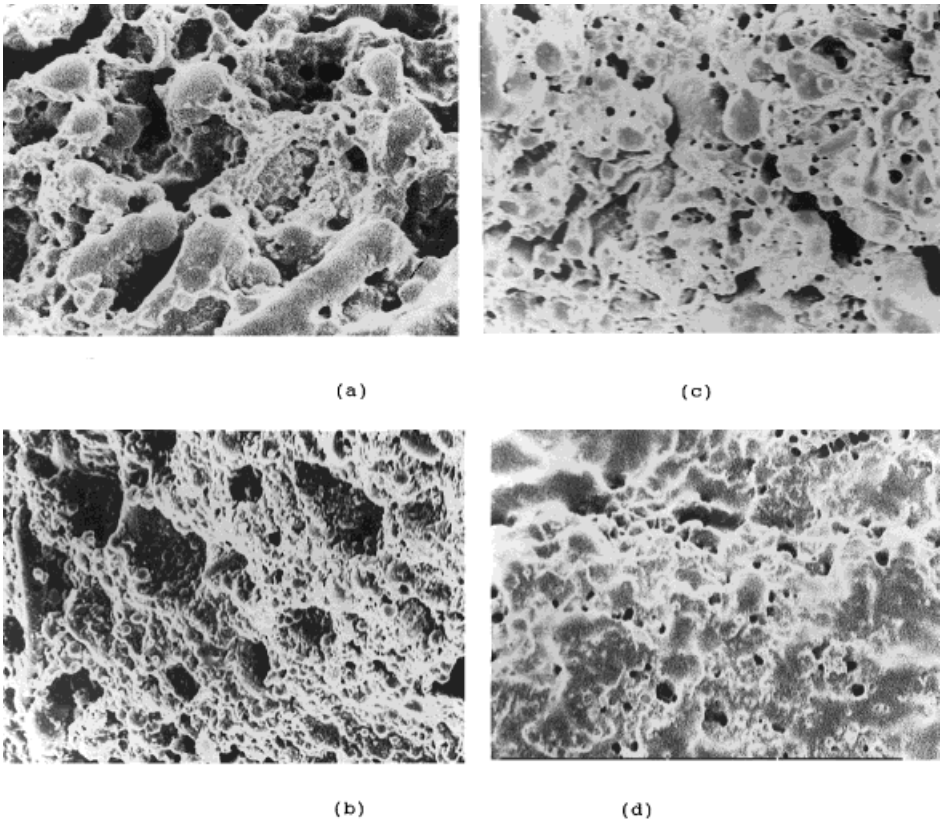

Figure 3 SEM photographs of extrudate of NR–PS blends (solution-cast) at different shear rates: (a) noncompatibilized at 57.6 s^{-1}, (b) noncompatibilized at 115.2 s^{-1}, (c) compatibilized at 57.6 s^{-1}, and (d) compatibilized at 115.2 s^{-1}).

where W_i is the weight fraction of the ith component of the blend. Immiscible blends are expected to show negative deviation, and miscible blends are expected to show a positive deviation. Different models can be used to calculate the viscosity of the blend. According to the series model,

$$\eta_{mix} = \eta_1\phi_1 + \eta_2\phi_2 \quad \text{(model 1)} \tag{6}$$

where η_1 and η_2 are the viscosities of component 1 and 2, and ϕ_1 and ϕ_2 are their volume fractions.

According to Hashin's upper and lower limit models, viscosity can be calculated as follows.

$$\eta_{mix} = \eta_2 + \frac{\phi_1}{1/(\eta_1 - \eta_2) + \phi_2/(2\eta_2)} \quad \text{(model 2)} \tag{7}$$

$$\eta_{mix} = \eta_1 + \frac{\phi_2}{1/(\eta_2 - \eta_1) + \phi_1/(2\eta_1)} \quad \text{(model 3)} \tag{8}$$

A free volume state model developed by Mashelkar and coworkers[26] can also be applied to

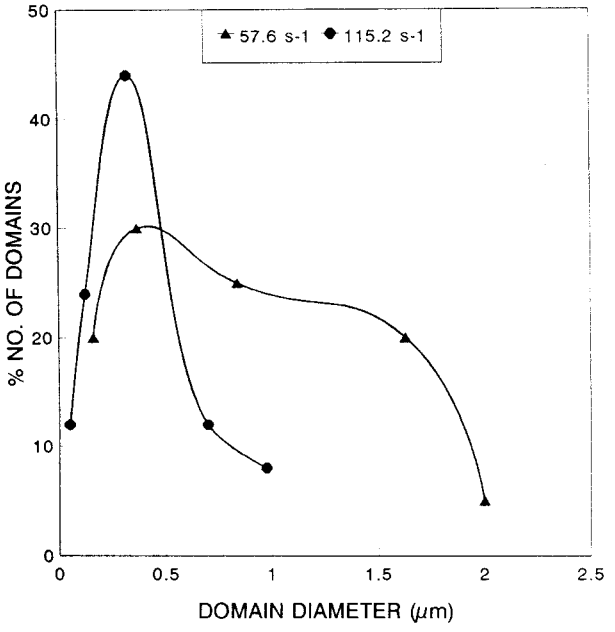

Figure 4 Distribution curves for 50/50 NR–PS blends in the absence of copolymer at different shear rates.

Table III Polydispersity Index Values of 50/50 NR–PS Blends at Different Shear Rates

Shear rate (s^{-1})	$\bar{D}_n$	$\bar{D}_W$	Polydispersity Index
57.6	0.78	1.22	1.57
115.2	0.36	0.54	1.50

compare with the experimental. According to this model,

$$\ln \eta_{mix} = \frac{\phi_1(\alpha - 1 - \gamma\phi_2)1n\ \eta_1 + \alpha\phi_2(\alpha - 1 + \gamma\phi_1)1n\ \eta_2}{\phi_1(\alpha - 1 - \gamma\phi_2) + \alpha\phi_2(\alpha - 1 + \gamma\phi_1)} \quad \text{(model 4)} \quad (9)$$

where η_1, η_2, ϕ_1, and ϕ_2 are the viscosities and volume fractions of the components 1 and 2, respectively. The α and γ values were calculated as explained in the literature.[26] Figure 7 shows the comparison between the experimental values and different theoretical models calculated at a shear rate of 230.4 s^{-1}. Up to 30 wt % NR, the experimentally observed values are found to be more close to the Mashelkar model, and, above 50 wt %, the experimental values are well below all the models.

Effect of Processing Conditions and Blend Ratio on Viscosity

Blends of NR and PS can be prepared either by the solution casting technique using chloroform as the casting solvent or by the melt mixing process in a Brabender plasticorder. The viscosity values are very much influenced by the method of preparation.

The effect of the blend ratio and the blending technique on shear viscosity can be understood from Figures 2 and 8. Solution-cast blends show a higher shear viscosity as compared to melt mixed samples (Table IV). This is further presented in Figure 5. Both in melt-mixed and solution-cast systems, the viscosity decreases with increase of shear stress, indicating pseudoplastic behavior. In both cases, negative and positive deviations in viscosity can be seen at a high and low shear rate. However, as compared to solution-cast blends, in melt-mixed ones, degradation of NR and PS due to high temperature and shear is possible. It is well known that both NR and PS undergo degradation under the application of high temperature and shear. The molecular weight values for NR and PS before and after the melt mixing process indicates that the component polymers have undergone considerable degradation during the melt mixing process. Before and after mixing, the values for $\bar{M}_n$ for NR were 7.79×10^5 and 4.70×10^5, respectively, and the values for PS were 3.51×10^5 and 2.08×10^5, respectively. This indicates extensive degradation of the material during melt mixing.

Effect of Compatibilizer Loading on Viscosity and Extrudate Morphology

The effect of compatibilizer loading on the shear viscosity of 50/50 NR–PS (solution-cast) at three different shear rates is given in Figure 9. As the compatibilizer loading increases, the shear viscosity increases, followed by a decrease at higher loading. The MFI measurements also showed a similar trend, as can be seen in the coming section. The initial increase in viscosity with copolymer loading indicates the higher interfacial interaction between the blend components at the interface.

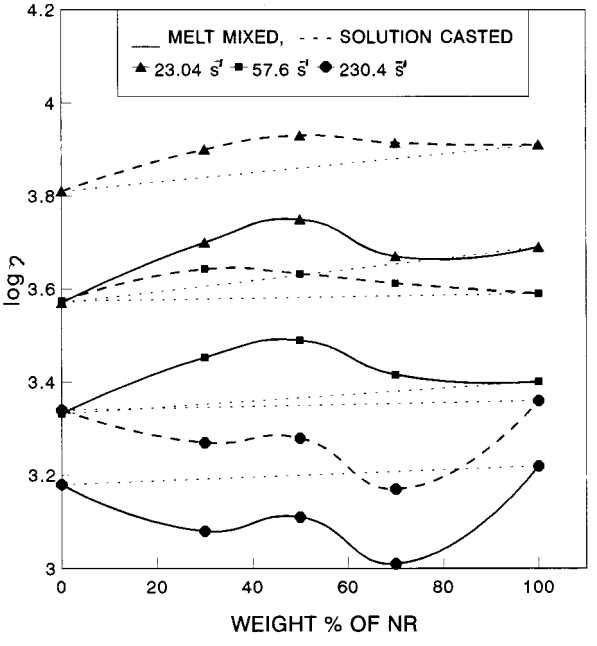

Figure 5 Variation of shear viscosity with weight percent of NR at different shear rates (solution-cast and melt-mixed).

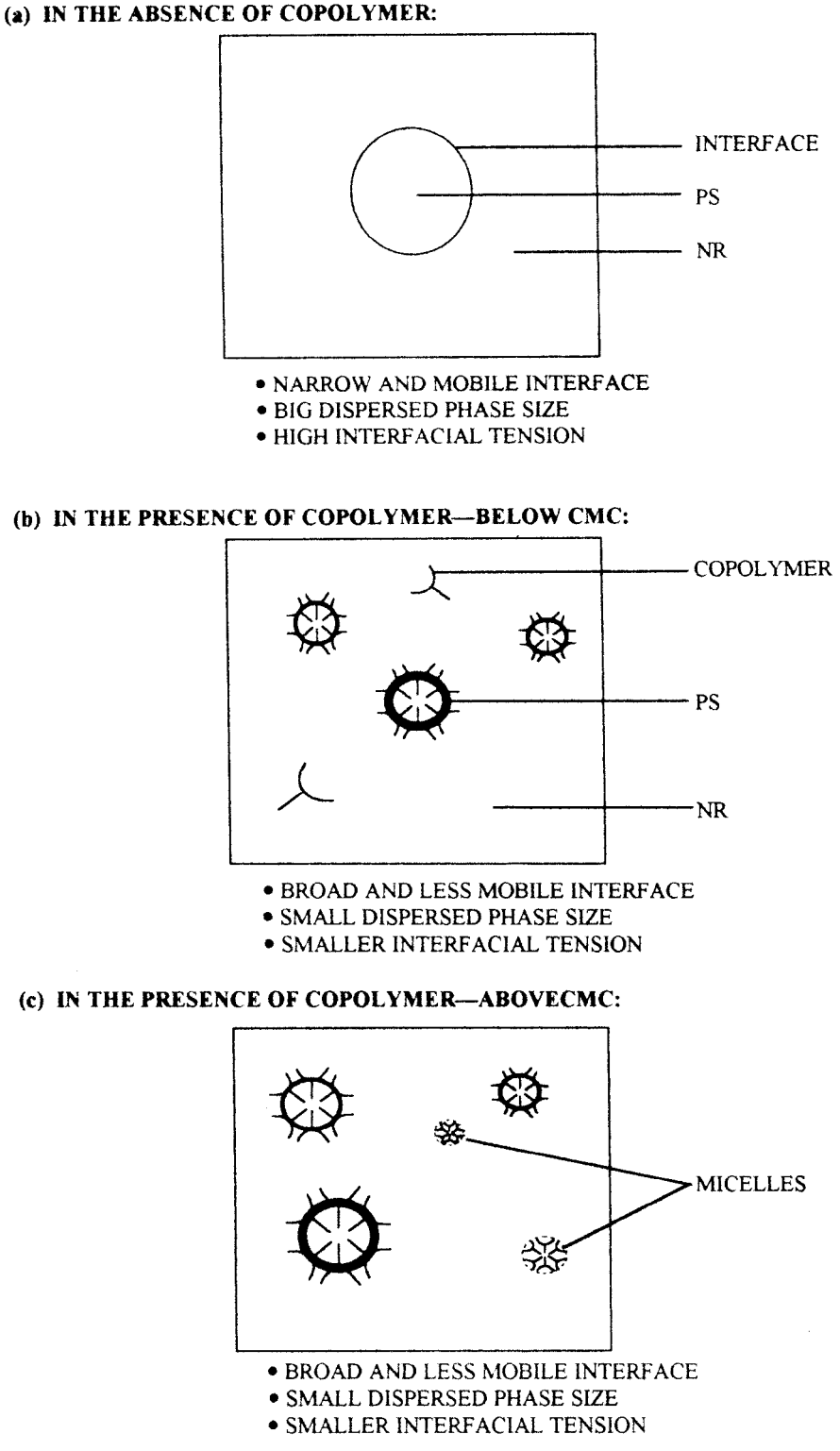

Figure 6 Schematic representation of the interface in the absence and presence of a compatibilizer (copolymer).

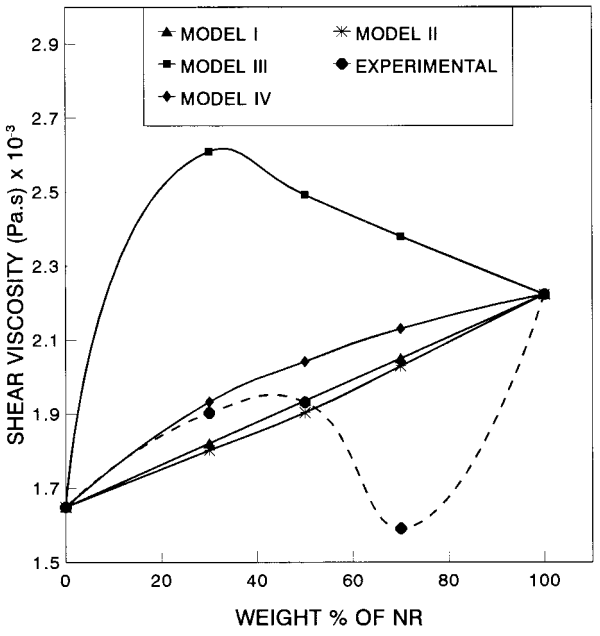

Figure 7 Experimental and theoretical values of shear viscosity as a function of weight percent of NR at 230.4 s^{-1}.

In fact, the compatibilizer decreases the interfacial tension, and the interaction between NR and PS is greatly enhanced. The graft copolymer locates at the blend interface and thereby holds the two phases together. The localization of the compatibilizer at the interface makes the interface less mobile, more broad, and stable. This has been schematically shown in Figure 6(b). Willis and Favis[27] reported an increase of viscosity upon the addition of a compatibilizer in immiscible binary blends. In the case of an incompatible blend, due to the presence of a sharp interface and poor interaction between the homopolymer phases, there occurs a high extent of inter layer slippage between the phases. Upon the addition of the graft copolymer, interfacial interaction between the phases increases, and there will be less slippage at the interface. Upon the addition of 3% graft copolymer, viscosity increases and, thereafter, it decreases at higher graft loading (Fig. 9). This is due to the fact that in the absence of the copolymer, NR–PS blend is highly incompatible, and the interface adhesion is very poor. The graft copolymer addition decreases the interfacial tension, and this leads to a reduction in the dispersed phase size and an increase in interfacial adhesion. In addition to the increase in interfacial adhesion, the presence of the graft copolymer at the blend interface broadens the interface region through penetration of the copolymer chains into the adjacent phases, which stabilizes the blend morphology against coalescence. Graft copolymer addition increases the interfacial adhesion, as evidenced by a decrease in the interfacial energy. The interfacial tension in NR–PS blend has been calculated using the following equation[28]:

$$\frac{G\eta_m a_n}{\gamma} = \left(\frac{4\eta_d}{\eta n_m}\right)^{0.84} \tag{10}$$

where G is the shear rate, γ is the interfacial tension, η_m and η_d are the viscosities of the continuous and dispersed phases, respectively, and a_n is the average size of the dispersed phase domains. It can be seen that the interfacial tension decreases with the increase of copolymer loading (Fig. 10).

The scanning electron microscopy (SEM) photographs of the extrudate cross section of NR–PS blends are given in Figure 11. Large dispersed domains are seen in 50/50 NR–PS blends in the absence of copolymer [Fig. 11(a)]. Upon the addition of the graft copolymer, the domain size decreases. The number-average domain size was measured and plotted the same against percentage graft copolymer added (Fig. 12). It can be seen

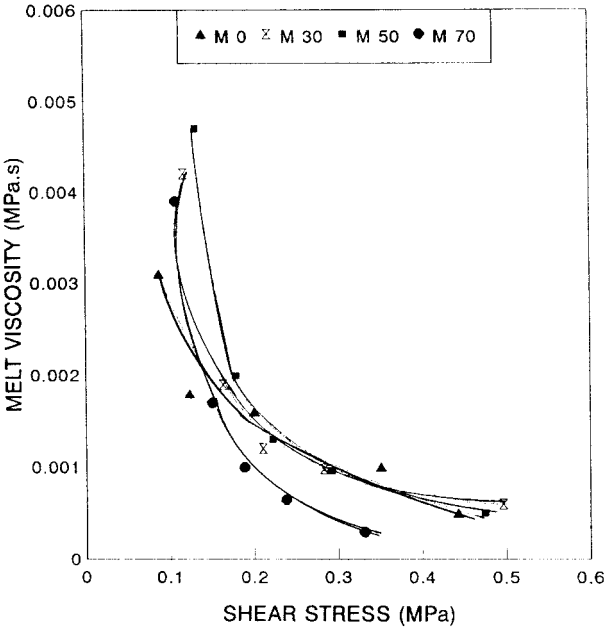

Figure 8 Variation of shear viscosity with shear stress of melt-mixed blends.

Table IV Shear Viscosity (Pa · s) of Melt- and Solution-Cast Samples

		Shear Rate			
Wt % of NR	Sample	23.04 s^{-1}	57.60 s^{-1}	230.40 s^{-1}	576 s^{-1}
30	Melt	5.11×10^3	2.83×10^3	1.23×10^3	8.46×10^2
	Solution	8.08×10^3	4.44×10^3	1.90×10^3	8.61×10^2
50	Melt	5.74×10^3	3.09×10^3	1.29×10^3	8.23×10^2
	Solution	8.79×10^3	4.36×10^3	1.93×10^3	8.40×10^2
70	Melt	4.68×10^3	2.60×10^3	1.03×10^3	5.75×10^2
	Solution	8.25×10^3	4.12×10^3	1.59×10^3	7.24×10^2

that there is a sharp decrease in diameter upon the addition of the compatibilizer followed by a leveling off at higher loading. The number-average domain size measurements were done by measuring the diameter of about 100 domains at random in each blend system. The interparticle distance also reduces by the addition of the compatibilizer, followed by leveling off at higher loading (Fig. 12). The interparticle distance was taken as the average distance between the centres of two neighboring domains. From these observations, we can calculate the optimum amount of compatibilizer required to saturate unit volume of the blend interface [called critical micelle concentration (CMC)]. The CMC value has been estimated by the intersection of the straight lines obtained at low concentration and leveling of line at higher concentration (Fig. 12) domain size versus copolymer loading and is found to be 1.8% for 50/50 NR–PS blend system. Beyond CMC, further addition of the compatibilizer makes no difference in the domain size and, hence, the interfacial tension.

Effect of Temperature and Shear Stress on Viscosity

The variation of shear viscosity with temperature of 50/50 NR–PS blends is given in Figure 13. It is clear that as the temperature increases from 150–160°C, the viscosity decreases both in melt-

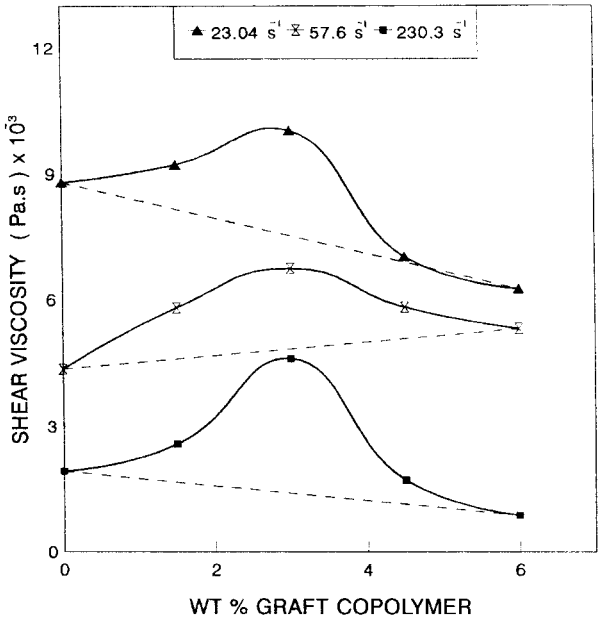

Figure 9 Variation of shear viscosity with the percentage of graft copolymer (50/50 NR–PS) solution-cast blends.

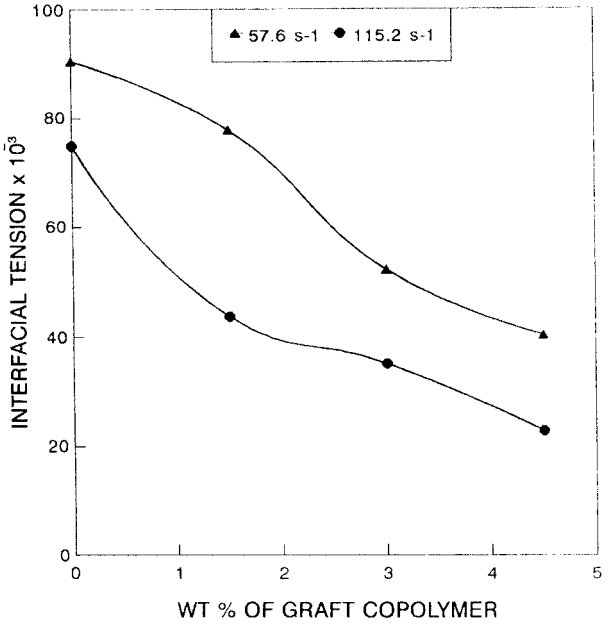

Figure 10 Reduction in interfacial tension upon graft loading.

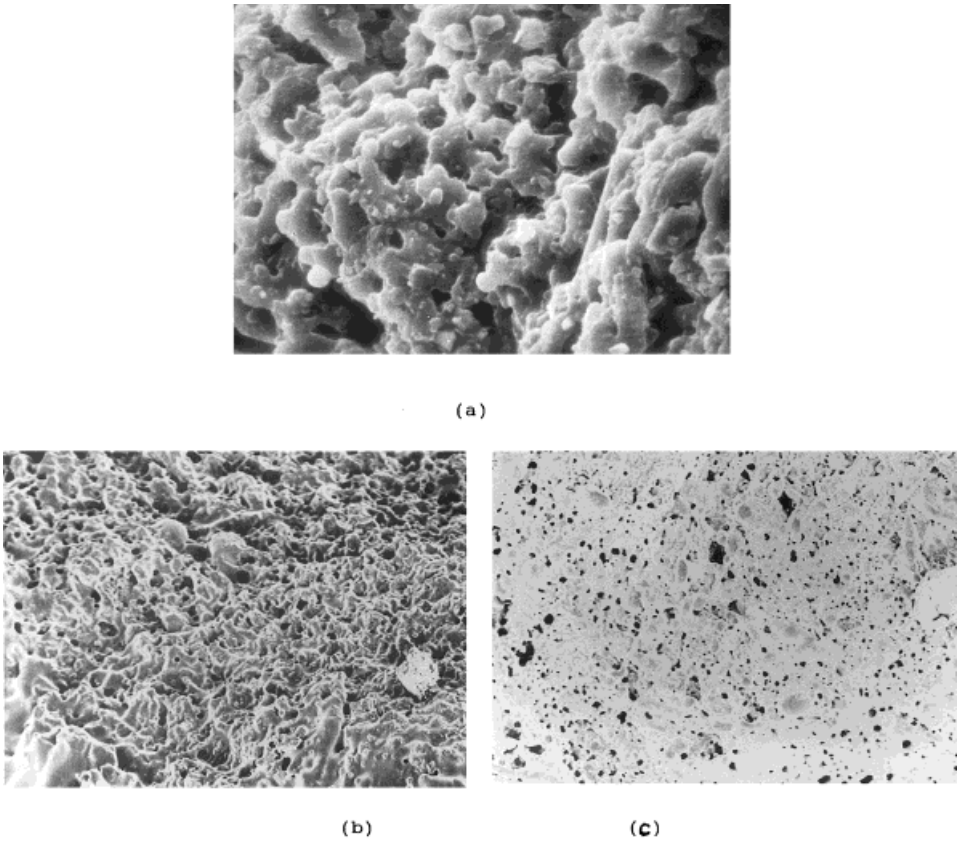

Figure 11 SEM photographs of extrudate of solution-cast 50/50 NR–PS blends: (a) 0, (b) 1.5, and (c) 3% graft copolymer.

mixed and solution-cast samples and thereafter increases. Effect of temperature on shear viscosity of compatibilized 50/50 NR–PS blends (solution-cast-graft loading, 4.5%) is also given in Figure 13. In this case too, shear viscosity decreases with temperature first and then increases at high temperature. As the temperature increases, the initial fall in viscosity is due to the degradation of the material and, thereafter, it increases because the system undergoes crosslinking at high temperature. Here also, the pseudoplasticity is maintained in all the samples. In order to understand further the influence of temperature on viscosity, Arrhenius plots at a constant shear rate were drawn (Fig. 14). In the Arrhenius plots, log η is plotted versus $1/T$. In the Arrhenius equation, η is related to the absolute temperature (T) by the following equation:

$$\eta = A_e - E/RT \tag{13}$$

where A is a constant characteristic of the polymer, E is the activation energy, and R is the universal gas constant. The Arrhenius plots of the samples at two different shear rates (23.04 and 230.45 s^{-1}) are given in Figure 14. The activation energies of blends calculated from the slopes of these plots are given in Table V. The activation energy of a material provides valuable information on the sensitivity of the material towards the change in temperature. The higher the activation energy, the more temperature sensitive the material will be. The activation energy of the solution-mixed sample is higher than the melt-mixed sample. By the addition of the compatibilizer, activation energy decreases. This means that the blends become less temperature-sensitive in the presence of the compatibilizer. Such information is highly useful in selecting the temperature for processing during the product manufacture.

Flow Behavior Index (n')

The effects of temperature and blend ratio on the flow behavior indices of the samples have been studied in detail. The extent of pseudoplasticity or non-Newtonian behavior of the materials can

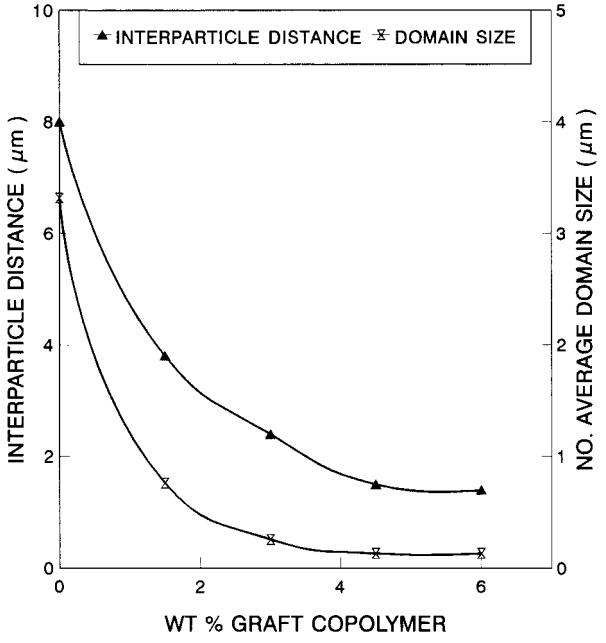

Figure 12 Variation of number-average domain diameter and interparticle distance as a function of graft copolymer concentration (50/50 NR–PS solution-cast blends).

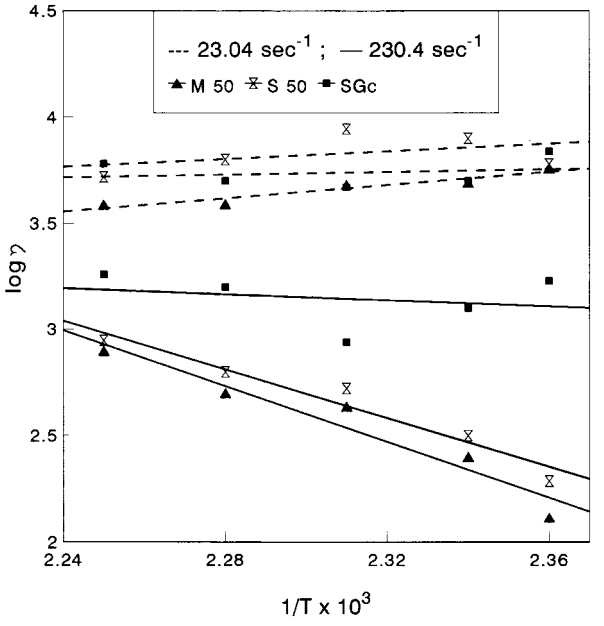

Figure 14 Arrhenius plots for different NR–PS blends (50/50 NR–PS solution-cast blends).

be understood from n' values. Pseudoplastic materials are characterized by n' below 1.

Flow behavior index values of NR–PS blends, both melt-mixed and solution-cast systems, are given in Table VI. All the mixes are non-Newtonian pseudoplastic fluids characterized by n' below 1. Flow behavior index value of PS is greater than that of NR both in melt and solution-cast samples. In both melt and solution-cast blends, as the amount of PS decreases, the value of n' decreases. Melt-mixed samples show a high value of n' compared to solution-cast ones at 150°C, and this is because during melt mixing, degradation may occur to the melt-mixed samples. This indicates a low pseudoplastic nature of the melt-mixed blend as compared to the solution-cast one. The effect of compatibilizer loading on the n' value of 50/50 NR–PS blends (solution-cast) are also given in Table VI. Here also, in all cases, the value of n' is below 1, indicating a non-Newtonian pseudoplastic nature. As the compatibilizer loading increases, the n' value increases. This suggests that the system becomes less pseudoplastic

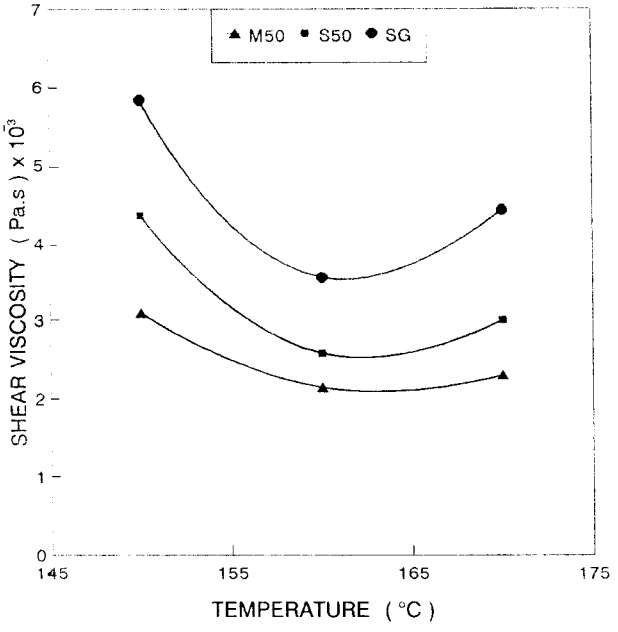

Figure 13 Effect of temperature on shear viscosity of different blends (50/50 NR–PS solution-cast blends).

Table V Activation Energy of Blends

Sample	Activation Energy (Cal/mol)
M_{50}	2242
S_{50}	4567
$SG_{(c)}$	3093

Table VI n' at 150°C

Melt Mixed		Solution Cast		Compatibilized	
M_0	0.4078	S_0	0.3171	0	0.2866
M_{30}	0.3682	S_{30}	0.2949	1.5	0.2942
M_{50}	0.3238	S_{50}	0.2866	3	0.3174
M_{70}	0.3060	S_{70}	0.2333	4.5	0.3743
M_{100}	0.2998	S_{100}	0.2019	6	0.3891

as compatibilizer loading increases. The effect of temperature on n' of 50/50 NR–PS blends is given in Table VII. Here also, melt-mixed samples show a high value for n' compared to solution-cast ones, and, as the temperature increases, the value of n' decreases in both cases. Hence, it can be concluded that the pseudoplasticity of NR–PS blends increases with an increase in the temperature and the weight percentage of NR. The effect of temperature on n' is the same as that of noncompatibilized NR–PS blends. A similar trend of decreasing values of n' with an increase in temperature has been reported elsewhere.[29,30]

Extrudate Deformation Studies

Figures 15 and 16 are the optical photographs of the extrudates, which show the deformation of the blends with and without the compatibilizer, respectively, at two different shear rates. Solution-cast blends show high distortion compared to melt-mixed samples both at low and high shear rate regions. Most of the extrudates have smooth surfaces at low shear rates. At high shear rates, the extrudate surface exhibits different degrees of distortion. This is associated with the melt fracture, which occurs at high shear forces where the shear stress exceeds the strength of the melt.[2] The presence of the compatibilizer reduces the extrudate deformation because it makes the blend more rigid and stronger.

Melt Elasticity

The important parameters that characterize the elasticity of polymer melts are die swell (d_e/d_c),

Table VII n' of 50/50 Blend

Temperature (°C)	Melt	Solution	SG_C
150	0.3238	0.2866	0.3743
160	0.2926	0.2387	0.3731
170	0.2614	0.1908	0.2754

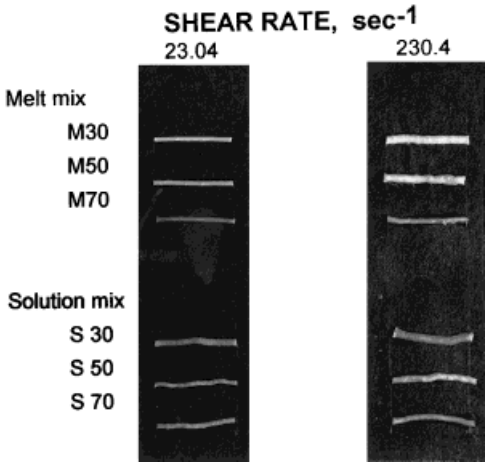

Figure 15 Extrudate deformation at different shear rates as a function of blend composition (50/50 NR–PS solution-cast blends).

principal normal stress difference (τ_{11}–τ_{22}), and recoverable elastic shear strain (S_R).

Die swell ratio (d_e/d_c) is the ratio of the extrudate diameter (d_e) to the diameter of the capillary (d_c). The principal normal stress difference (τ_{11}–τ_{22}) is calculated from the die swell and shear stress according to Tanner's equation as follows.[31]

$$\tau_{11} - \tau_{22} = 2\tau_w[2(d_e/d_c)^6 - 2]^{1/2} \qquad (14)$$

Recoverable elastic shear strain (S_R) is given by the following equation:

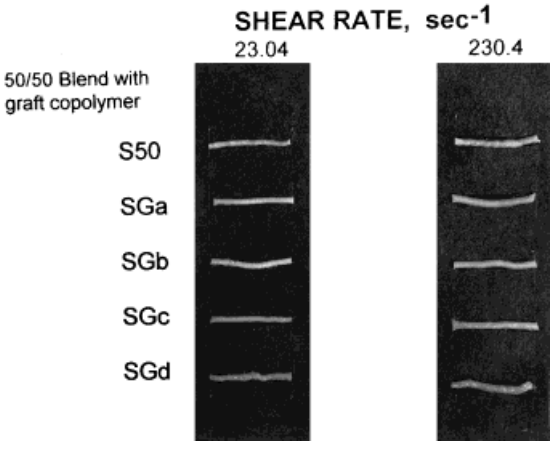

Figure 16 Extrudate deformation at different shear rates as a function of compatibilizer loading (50/50 NR–PS solution-cast blend).

Table VIII Die Swell Value at 150°C

Shear Rate (s^{-1})	M_{30}	M_{50}	M_{70}	S_{30}	S_{50}	S_{70}	SG_a	SG_b	SG_c
2.304×10^1	1.35	1.36	1.30	1.82	1.45	1.56	1.57	1.58	1.55
2.304×10^2	2.31	2.06	1.45	2.24	1.84	1.61	1.87	1.79	1.71

$$S_R = (\tau_{11} - \tau_{22})/2\tau_w \quad (15)$$

Die Swell

Table VIII shows the die swell ratio of the melt-mixed, solution-cast, and compatibilized NR–PS blends at two shear rates at 150°C. For all the mixes, the die swell increases with an increase in shear rate. Within the capillary, the molten polymer under shear will maintain orientation of the polymer chains and when it emerges from the die, recoiling of chains occurs, leading to the phenomenon of die swelling. This phenomenon is due to the relaxation imposed in the capillary and to factors like chain breaking, stress relaxation, crosslinking, presence of fillers, and plasticizers, which control the elastic recovery. The effect of temperature on the die swell value of 50/50 NR–PS blends is given in Table IX. Both in melt-mixed and solution-cast blends, the die swell increases with an increase of temperature; whereas in the compatibilized system, the die swell decreases with an increase of temperature. Comparing solution-cast and melt-mixed samples, at a lower shear rate, solution-cast blend shows a higher value of d_e/d_c due to the high molecular weight of NR in the blend. But at a higher shear rate, the reverse trend is obtained because of the molecular break down of NR. In both melt-mixed and solution-cast blends, as the amount of NR increases, the value of d_e/d_c decreases in most cases. In most cases, the die swell values decrease with compatibilizer loading (Tables VIII and IX). This is due to the fact that the interface becomes stronger as a result of the addition of compatibilizer.

Table IX Die Swell at Shear Rate of 23.04 s^{-1}

Temperature (°C)	M_{50}	S_{50}	SG_c
150	1.36	1.45	1.55
160	1.48	1.52	1.49
170	1.51	1.75	1.43

Principal Normal Stress Difference (τ_{11}–τ_{22})

Table X shows the value of principal normal stress difference of melt-mixed, solution-cast, and compatibilized blends at 150°C and at a shear rate of 23.04 s^{-1}. Both in melt-mixed and solution-cast blends, the principal normal stress difference decreases with an increase in the rubber content. Values are higher for solution-cast samples compared to the corresponding melt-mixed ones. The incorporation of the compatibilizer decreases the principal normal stress values. In fact, the higher values of normal stress difference indicate greater elastic recovery or high melt elasticity. Upon the addition of the compatibilizer, the blend becomes less deformable and, hence, produces greater resistance to flow; that is, it exhibits a higher melt viscosity. The effect of temperature on principal stress difference is given in Table XI. The values decrease with the increase of temperature for both melt-mixed and solution-cast blends. In the case of compatibilized blends, the

Table X Melt Elasticity Values at 150°C[a]

Sample	Principal Normal Stress Difference (τ_{11}–τ_{22}) (N/m^2)	Recoverable Shear Strain (S_R)
M_{30}	99.05×10^5	17.48
M_{50}	73.31×10^5	12.31
M_{70}	19.38×10^5	4.07
S_{30}	139.80×10^5	15.93
S_{50}	78.07×10^5	8.76
S_{70}	42.24×10^5	8.76
$SG_{(a)}$	67.26×10^5	9.21
$SG_{(b)}$	59.57×10^5	7.98
$SG_{(c)}$	48.33×10^5	13.59
$SG_{(d)}$	20.65×10^5	9.43

[a] Shear rate is 23.04 s^{-1}.

Table XI Effect of Temperature on Melt Elasticity

Sample	Temperature (°C)	Principal Normal Stress ($\tau_{11}-\tau_{22}$) (N/m^2)	Recoverable Shear Strain (S_R)
M_{50}	150	73.31×10^5	12.31
	160	41.77×10^5	9.36
	170	25.28×10^5	6.92
S_{50}	150	78.07×10^5	8.76
	160	47.81×10^5	7.71
	170	24.71×10^5	6.04
$SG_{(c)}$	150	48.33×10^5	13.59
	160	22.14×10^5	6.95
	170	30.81×10^5	7.64

values decrease with temperature up to 160°C and, thereafter, decrease.

Recoverable Shear Strain

Recoverable shear strain, a measure of the elastic energy stored in the system is given in Table X. The excess energy stored may be converted to surface free energy, which leads to extrudate deformation.[10] The behavior of S_R is the same as that of principal normal stress difference, except in the case of compatibilized systems. In the case of compatibilized systems, S_R decreases first, then increases, and finally decreases at high graft loading. The effect of temperature is the same as that of principal normal stress differences.

Melt Flow Index

The melt flow index provides valuable information about the flow behavior of materials. Table XII shows the MFI values of melt-mixed, solution-cast, and compatibilized 50/50 NR–PS blends. MFI experiments were done at 250°C. It is found that MFI values decrease with an increase of rubber content both in melt-mixed and solution-cast samples. Solution-cast samples show lower values as compared to melt-mixed samples. This is because in solution-cast samples, viscosity is higher as compared to melt-mixed samples. As the viscosity increases, the MFI value decreases. These results are in agreement with the capillary rheometer data. It is already seen that in the case of compatibilized blends, viscosity increases upon the addition of graft copolymer (up to 3 wt %), and, thereafter, it decreases. MFI values of compatibilized blends support this trend. MFI values decrease with increases of graft loading up to 3 wt % graft copolymer, then it increases with an increase in graft copolymer loading.

Shenoy et al.[32] developed a method to estimate the rheograms from a knowledge of MFI of the material. Bhagawan et al.[33] combined the MFI and capillary rheometer data to provide master curves for silica-black-filled thermoplastic IIR, polybutadiene rubber. Figures 17 and 18 show the master curves of the blends obtained by the correlating MFI and capillary rheometer data for the compatibilized and non-compatibilized blends. Using a plot of ($\log \eta \times \mathrm{MFI}/\rho$) versus ($\log \rho\dot{\gamma}/\mathrm{MFI}$) (where ρ is density of the blend; it is shown that the various curves were unified as a single master curve. This suggests that by simply knowing the MFI of the sample, rheograms of any system can be constructed using the master curve.

Table XII Melt Flow Index of Blends at 250°C

Sample	M_{30}	M_{50}	M_{70}	S_{30}	S_{50}	S_{70}	$SG_{(a)}$	$SG_{(b)}$	$SG_{(c)}$
MFI (g/10 min)	2.2086	2.1898	1.7814	1.482	1.376	0.602	0.716	0.651	1.237

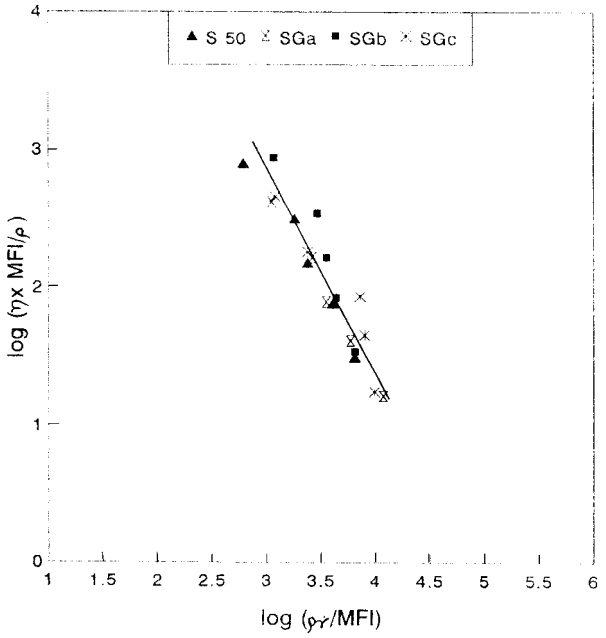

Figure 17 Master curve of modified shear viscosity versus modified shear rate for the compatibilized system (50/50 NR–PS solution-cast blends).

CONCLUSION

Melt rheological properties of NR–PS blends have been investigated using a capillary rheometer and melt flow indexer. Blends were prepared by both melt mixing and solution casting techniques. In both cases, the shear viscosity decreased with the increase of shear stress, indicating pseudoplastic nature. The viscosity of the system was found to increase with the increase of the rubber content. The solution-cast blends showed higher viscosity as compared to melt-mixed samples. Mechanical degradation of both NR and PS at high temperature and shear have contributed to the lower viscosity of melt blended samples. At the lower shear rate region, the viscosities of the blend are higher than those of the component polymers (positive deviation). On the other hand, at high shear rate, the system exhibits a negative deviation. Morphology analysis revealed that the dispersed domain size has been reduced significantly at high shear rate. Various theoretical models have been used to fit the experimental viscosity data. Melt viscosity of the blends increases upon the addition of a few percent of the compatibilizer (NR-*g*-PS) followed by a decrease at higher loading. The increase in viscosity has been explained on the basis of the high interfacial interaction between the component polymers. The micelle formation is believe to be responsible for the decrease in viscosity at higher graft loading. The SEM analysis of the extrudate cross-section indicated that the domain size and interparticle distance decrease with increase of copolymer loading and finally get leveled off at higher copolymer loading. Arrhenius plots and activation energy measurements give information about the temperature dependence of different blend systems.

Melt elasticity parameters like die swell, principal normal stress differences, and recoverable shear strain were calculated for both compatibilized and noncompatibilized blends. Melt flow index studies are in agreement with the capillary rheometer data. Finally, master curves have been constructed using the MFI and rheometer data for both the compatibilized and uncompatibilized both blends.

The authors thank Dr. Rani Joseph and Dr. Philip Kurian, Department of Polymer Science and Technology, Cochin University of Science and Technology, for their help in the rheological analysis. One of the authors (RA) thanks the Council of Scientific and Industrial Research (CSIR) for the award of the Senior Re-

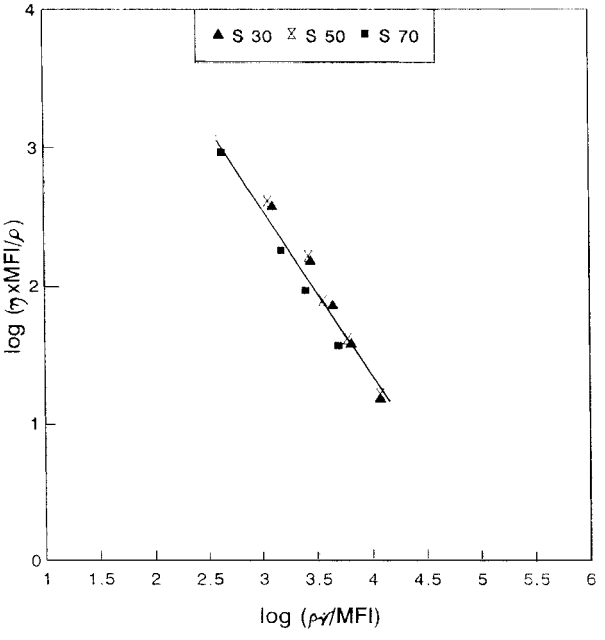

Figure 18 Master curve of modified shear viscosity versus modified shear rate as a function of blend composition (50/50 NR–PS solution-cast blends).

search Fellowship. Thanks are also due to Department of Science and Technology (DST), New Delhi, for financial assistance.

REFERENCES

1. R. Asaletha, M. G. Kumaran, and S. Thomas, *Rubber Chem. Technol.,* **68,** 671 (1995).
2. J. A. Brydson, *Flow Properties of Polymer Melts,* 2nd ed., George Godwin Ltd., London, 1981.
3. S. Danesi and R. S. Porter, *Polymer,* **19,** 448 (1978).
4. S. Akhtar, B. Kuriakose, Prajna P. De, and S. K. De, *Plast. Rubber Process. Appl.,* **7,** 11 (1987).
5. A. K. Gupta, A. K. Jain, and S. N. Maiti, *J. Appl. Polym. Sci.,* **38,** 1699 (1989).
6. A. T. Koshy, B. Kuriakose, S. Thomas, C. K. Premaletha, and S. Varghese, *J. Appl. Polym. Sci.,* **49,** 901 (1993).
7. Y. J. Kim, G. S. Shir, I. T. Lee, and B. K. Kein, *J. Appl. Polym. Sci.,* **47,** 295 (1993).
8. C. S. Ha, *J. Appl. Polym. Sci.,* **35,** 2211 (1988).
9. H. Vanoene, *J. Colloid Interface Sci.,* **40,** 448 (1972).
10. L. A. Goettler, J. R. Richwine, and F. J. Wille, *Rubber Chem. Technol.,* **55,** 1448 (1982).
11. Y. Germain, B. Ernst, O. Genelot, and K. Dhamani, *J. Rheol.,* **38,** (1994).
12. A. K. Gupta and S. N. Purwar, *J. Appl. Polym. Sci.,* **30,** 1778 (1985).
13. A. Valenza and D. Acierno, *Eur. Polym. J.,* **30,** 1121 (1994).
14. R. M. H. Miettinen, J. V. Seppala, O. T. Ikkala, and I. T. Reima, *Polym. Eng. Sci.,* **34,** 5 (1994).
15. M. Joshi, S. N. Maiti, and A. Misra, *J. Appl. Polym. Sci.,* **45,** 1837 (1992).
16. L. A. Utracki and P. Sammut, *Polym. Eng. Sci.,* **17,** 30, 1027 (1990).
17. Z. Oommen, C. K. Premaletha, B. Kuriakose, and S. Thomas, *Polymer,* **38,** 5611 (1997).
18. W. Cooper, P. R. Sewell, and G. Vaughan, *J. Polym. Sci.,* **41,** 167 (1959).
19. M. Goni, G. Chaga, J. S. Roman, M. Valero, and G. M. Guzman, *Polymer,* **34,** 512 (1993).
20. H. Munstedt, *Polym. Eng. Sci.,* **5,** 21, 259 (1981).
21. L. A. Utracki, *Polym. Eng. Sci.,* **23,** 602 (1983).
22. T. S. Lee, in *Proceedings of the 5th International Conference on Rheology,* Vol. 4, University Park Press, Baltimore, 1970, p. 421.
23. T. I. Ablasova, *J. Appl. Polym. Sci.,* **19,** 1781 (1975).
24. T. Fujimura and K. Iwakura, *Kobunshi Roubunsbu,* **31,** 617 (1974).
25. S. K. Khanna and W. I. Congdon, *Polym. Eng. Sci.,* **23,** 627 (1983).
26. R. Sood, M. G. Kulkarni, A. Dutta, and R. A. Mashelkar, *Polym. Eng. Sci.,* **28,** 20 (1988).
27. J. M. Willis and B. D. Favis, *Polym. Eng. Sci.,* **28,** 1416 (1988).
28. S. Wu, *Polym. Eng. Sci.,* **27,** 335 (1987).
29. S. Thomas, B. Kuriakose, B. R. Gupta, and S. K. De, *Plast. Rubber Process Appl.,* **6,** 85 (1986).
30. D. R. Saini and A. V. Shenoy, *J. Macromol. Sci., Phys.,* **B22,** 437 (1983).
31. R. I. Tanner, *J. Polym. Sci. A-Z,* **14,** 2067 (1970).
32. A. V. Shenoy, S. Chattopadhyay, and V. M. Nadkarni, *Rheol. Acta,* **22,** 90 (1983).
33. S. S. Bhagawan, D. K. Tripathy, and S. K. De, *Polym. Eng. Sci.,* **28,** 448 (1988).